European Journal of Orthodontics 18 (1996) 655–662

The extent of enamel surface fractures. A quantitative comparison of thermally debonded ceramic and mechanically debonded metal brackets by energy dispersive micro- and image-analysis

U. Stratmann*, K. Schaarschmidt**, H. Wegener*** and U. Ehmer***

*Institute of Anatomy, **Clinic of Pediatric Surgery, ***Clinic of Dentistry, Division of Orthodontics, University of Münster, Germany

SUMMARY This clinical study investigated the practical value of two methods for debonding brackets attached by the adhesive Concise to acid-etched enamel surfaces. Forty-two Ultratrimm Standard metal brackets and 42 Fascination ceramic brackets were collected from juvenile patients undergoing orthodontic treatment. All metal brackets were mechanically debonded by a conventional bracket removal plier, whereas the ceramic brackets were thermally debonded by a commercial Dentaurum ceramic debonding unit. All brackets were evaluated by scanning electron microscopy for the morphology of their adhesive fracture surfaces and for the occurrence of mineral-like particles attached to the adhesive fracture surfaces. These particles were analysed by an energy dispersive X-ray microprobe for their Ca/P ratios and by image analysis of scanning electron micrographs for measurement of their areas. The scanning electron micrographs showed 4 types of debonding fractures. The most frequent fracture was type 1 (between adhesive and bracket base) and type 2 (between adhesive and enamel surface). In the group of mechanically debonded metal brackets type 1 (38 per cent) and type 2 (45 per cent) showed a similar fequency, whereas thermally debonded ceramic brackets predominantly showed fracture type 1 (79 per cent) and only a minor percentage of type 2 (11 per cent). A statistical evaluation was applied to estimate the range of reproducibility of fracture types with a 95 per cent confidence interval (level of significance $\alpha = 5$ per cent). In both groups the microprobe analysis of fracture surfaces lying completely or partly between adhesive and enamel surface identified the mineral-like particles as enamel mineral. They occurred partly as single particles (range of thickness: 5–25 μm, mean area: 3500 μm^2) and partly as a coherent covering with a total area of 1.9–5.8 mm^2.

It is concluded that the thermodebonding technique is superior to conventional mechanical debonding, because the frequent occurrence of fracture type 1 after thermodebonding affords a protection for the enamel surface, whereas mechanical debonding entails a comparatively high risk of enamel fractures.

Introduction

In orthodontic treatment of adults higher aesthetic demands for orthodontic appliances have to be considered compared with those in the treatment of children (Hertrich and Hirschfelder, 1990). Plastic brackets are inconspicuous but have only a limited range of indications due to their mechanical limitations. Ceramic reinforced plastic brackets seem to outweigh many of these disadvantages but have only recently been introduced, so that clinical experience is still limited. Therefore the aesthetically exacting patient is frequently supplied with ceramic brackets, which entail some major problems. Firstly an increased abrasion of antagonist teeth due to the considerable hardness of the ceramic material has been proven in clinical studies (Douglas, 1989) and in

experimental investigations (Newesely and Rossiwall, 1989). Secondly the risk of enamel fracture is particularly high during mechanical debonding, since the fracture interface frequently lies between adhesive and enamel surface (Ødegaard and Segner, 1988). According to Bishara and Trulove (1990) this risk is additionally increased after extensive endodontic treatment. Thirdly Scott (1988) and Kusy (1988) have pointed out that the high elastic modulus of ceramic brackets has a risk of breaking the bracket itself, as conventional methods of mechanical debonding seem to subject the fragile material to excessive shear and traction forces.

Consequently the need for a safer method with a more controlled mode of debonding and thus a reduced incidence of bracket and enamel fractures arises particularly for debonding of ceramic brackets. For this purpose modifications of different enamel conditioning agents (Maskeroni *et al.*, 1990) or varying adhesive systems have been evaluated. More recently ceramic brackets have been debonded thermally according to a technique decribed by Sheridan *et al.* (1986) for metal brackets.

The aim of the present study was to investigate the morphology of the fracture surface after thermally processed debonding of ceramic brackets in comparison with mechanically debonded metal brackets. This study focussed in detail on the detection and the morphometric determination of enamel fractures after debonding.

Materials and methods

For this investigation 42 Fascination ceramic brackets (Dentaurum Ltd., Pforzheim Germany) from juvenile patients (12–16 years of age) were available after termination of orthodontic treatment of 1.5 years on average. All brackets had been debonded from the labial surfaces of permanent incisors by an apparatus specially designed for thermodebonding of ceramic brackets (ceramic debonding unit; Dentaurum Ltd.), which was equipped with a metallic element for insertion into the bracket slot. Heating of the element was achieved by an impulse voltage (2–2.2 V) applied for a period of 3 seconds, which was accompanied by a slight torque for removing the bracket.

The control group consisted of 42 Ultratrimm Standard metal brackets (Dentaurum Ltd.) mechanically debonded from the buccal surfaces of first and second permanent molars by a conventional bracket removal plier after orthodontic treatment of juvenile patients for comparable periods. Both the metal and ceramic brackets had been attached to acid etched tooth surfaces (37 per cent H_3PO_4, 60 seconds) by use of the Two-Paste-System Concise Orthodontic Bonding (3M Ltd., Neuss Germany). After gold sputtering (0.05 mbar, 1.5 minutes, thickness of gold layer: 30 nm) all brackets were evaluated by scanning electron microscopy at 25 kV. Morphologically notable mineral-like particles attached to the adhesive fracture surface as well as the particle-free adhesive fracture surfaces were analysed for their elemental composition by an energy dispersive X-ray microprobe (EDAX-Detecting Unit, Econ P 500x-149) coupled to the scanning electron microscope according to a method reported elsewhere (Ruppenthal *et al.*, 1992). All adhesive fracture surfaces were documented by survey and detailed scanning electron micrographs. Subsequently the negatives of the micrographs were digitized and the data were entered into an automatic image enhancement and image analysing system (IBAS, Contron Ltd., Düsseldorf, Germany) equipped with a morphometric program for planimetry (area measurement). The area of the enamel particles as well as the area of the adhesive fracture surface was determined and the percentage of the total particle area in relation to the total adhesive area was calculated. For statistical evaluation, a test was applied for estimating the range of reproducibility of fracture types and rates with a 95 per cent confidence interval (level of significance $\alpha = 5$ per cent).

Results

The evaluation of the scanning electron micrographs allowed determination of the precise course of the debonding fracture. In the group of thermally debonded ceramic brackets as well as in the group of mechanically debonded metal brackets four types of debonding fractures could be classified:

1. Fracture interface lying between adhesive and bracket base (type 1).
2. Fracture interface lying between adhesive and enamel surface (type 2).

Table 1 Distribution of debonding fracture types in the group of thermodebonding (group 1) and the group of mechanical debonding (group 2). Figures in parentheses are precentages.

	Type 1	Type 2	Type 3	Type 4
Group 1	33 of 42 (79)	5 of 42 (11)	2 of 42 (5)	2 of 42 (5)
Group 2	16 of 42 (38)	19 of 42 (45)	3 of 42 (7)	4 of 42 (10)

3. Fracture interface lying partly between adhesive and enamel surface and partly within the adhesive (type 3).
4. Fracture interface lying partly between adhesive and enamel surface, partly within the adhesive and partly between adhesive and bracket base (type 4).

Microanalysis of mineral-like particles

The evaluation of the microprobe X-ray spectra generated from mineral-like particles attached to the adhesive fracture surfaces (Figure 1) allowed a semi-quantitative analysis of element ratios after application of a mathematical correction of the count rates, i.e. the continuum method according to Hall (1971). All particle measurements provided Ca/P ratios with typical values of biological hydroxyapatite (Ca/P_{molar}: 1.51–1.67) and could therefore be identified as enamel mineral.

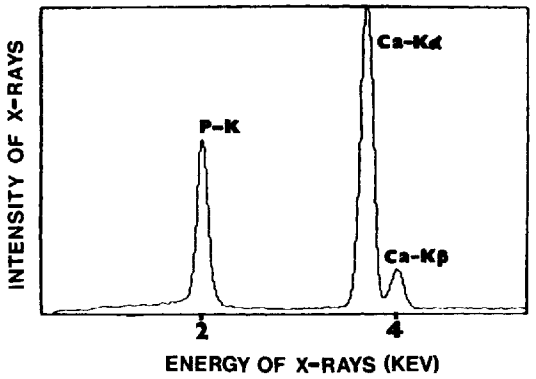

Figure 1 X-ray spectrum of a mineral-like particle attached to an adhesive fracture surface. P–K = X-radiation peak emerging from the K-shell of the element phosphorus, $Ca–K_{\alpha/\beta}$ = X-radiation peaks (consisting of a strong α-peak and a weak β-peak) emerging from the K-shell of the element calcium.

Table 2 Statistical estimation of expected percentages of the different fracture types (level of significance $\alpha = 5$ per cent).

Fracture type	Mechanical debonding	Thermodebonding
1	23–54	63–89
2	29–61	4–25
3	1.5–19	0.6–16
4	2.6–22	0.6–16

Thermodebonding of ceramic brackets

Table 1 gives the distribution of debonding fracture types in the group of thermodebonding. The results of the statistical estimation are given in Table 2. The microprobe analysis of fracture interfaces lying completely or partly between adhesive and enamel surface (types 2, 3 and 4) detected torn-out enamel particles attached to the adhesive in five out of eight specimens (62.5 per cent). In scanning electron micrographs most enamel fractures were visible at low magnification (Figure 2). Morphologically these particles occurred partly as single particles of varying shape, size and number and partly as a coherent covering with a predominantly serrated contour (Figure 3). High magnification revealed a prismatic morphology of the enamel particles (Figure 4). The regions of the adhesive

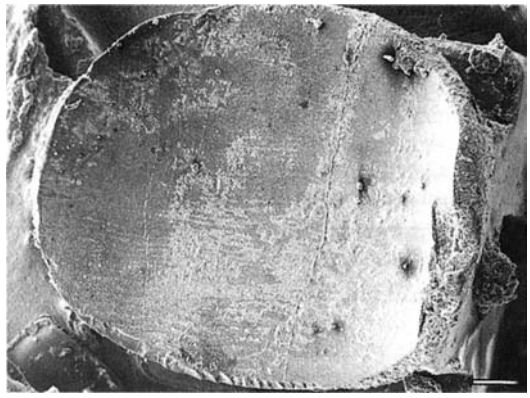

Figure 2 Scanning electron micrograph of an adhesive fracture surface of fracture type 2 (ceramic bracket, thermodebonding) with attached enamel particles. Bar = 330 μm.

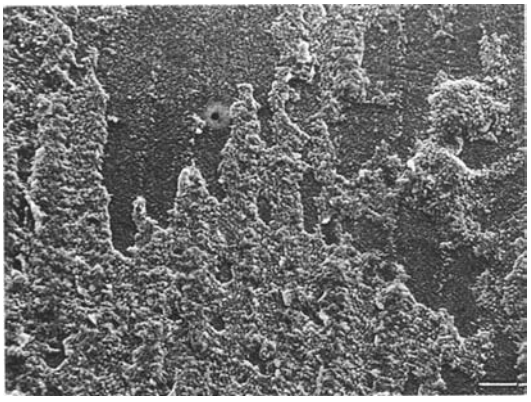

Figure 3 Scanning electron micrograph of an adhesive fracture surface of fracture type 2 (ceramic bracket, thermodebonding) with attached covering of coherent enamel particles. Bar = 50 μm.

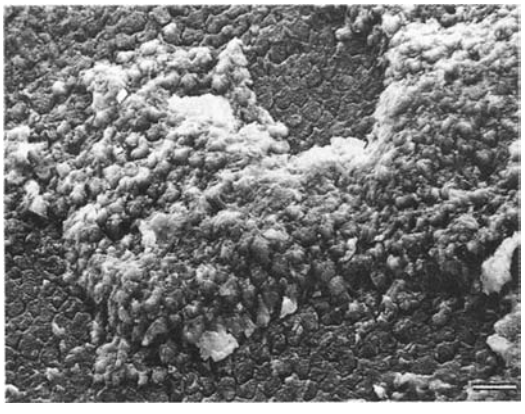

Figure 4 Scanning electron micrograph of an adhesive fracture surface of fracture type 2 (ceramic bracket, thermodebonding) with an attached prismatic enamel particle. Note the pattern of disrupted tag residues surrounding the enamel particle. Bar = 10 μm.

fracture surface neighbouring the enamel particles showed a pattern of tag residues (mean diameter = 5 μm), which had apparently been disrupted at their base during the thermodebonding process (Figure 4). The X-ray spectra of these features displayed pure Si-peaks, which afford additional evidence that they consist of adhesive substance without any enamel deposits. Silicon is a component of the anorganic microfilling of the adhesive and does not occur in enamel. The data of the morphometric analysis of the five specimens with enamel fractures are presented in Table 3.

The scanning electron micrographs did not allow a precise measurement of enamel particle thickness in the *Z*-axis, but it was estimated to lie in the range of 5–25 μm.

In contrast, in most specimens of type 1 debonding fracture the adhesive remnants bound to the bracket base showed a completely different morphology, which could be described as an irregular network of protrusions with a smooth and glossy appearance (Figure 5).

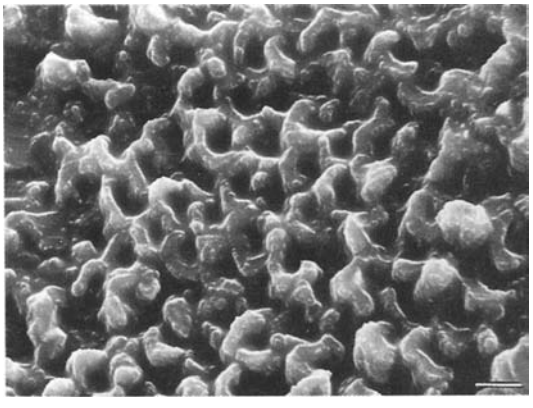

Figure 5 Scanning electron micrograph of an adhesive fracture surface of fracture type 1 (ceramic bracket, thermodebonding) with an irregular smooth and glossy morphology. Bar = 5 μm.

Table 3 Computer-aided area analysis of enamel particles and percentage of total particle area related to the total adhesive area after thermodebonding of ceramic brackets.

Specimen	Mean area of single enamel particle (μm²)	Total area of enamel particles (mm²)	Percentage of enamel particle area
1	3236	2.6	46
2	3452	1.9	27
3	*	5.8	37
4	4536	2.4	32
5	*	4.1	44

* Single enamel particles could not be detected.

Mechanical debonding of metal brackets

Table 1 gives the distribution of debonding fracture types in the group of mechanical debonding. The results of the statistical estimation are given in Table 2. The microprobe analysis of fracture interfaces lying completely or partly between adhesive and enamel surface (types 2, 3 and 4) detected torn-out enamel particles attached to the adhesive in 20 out of 26 specimens (77 per cent). As in the thermodebonding group most enamel fractures were visible at low magnification. At high magnification these occurred partly as single particles (Figure 6) of varying shape, size and number, and partly as a coherent covering as described above for the ceramic brackets.

Another frequent observation of the adhesive fracture surfaces neighbouring the enamel particles was a regular pattern of tag residues (mean diameter = 5 μm), which had obviously been disrupted in their basal portions during the mechanical debonding process (Figure 7).

The data of the morphometric analysis of the 20 specimens with enamel fractures are presented in Table 4. The estimate of the particle thickness corresponded to that after thermodebonding.

Discussion

The exact fracture mechanism during thermal debonding has not been previously elucidated. Most authors (Sheridan *et al.*, 1986; Gerkhardt *et al.*, 1988; Jost-Brinkmann *et al.*, 1989) assume the rapid temperature rise and the concomitant thermal expansion of the material cause structural tensions of the adhesive in the vicinity of the bracket base, whereas Bishara and Trulove (1990) attributed the fracture mechanism to a direct break of chemical bonds between the silane layer of the ceramic bracket base and the resin molecules, which they deemed to be due to the different thermal expansion coefficients of these two materials.

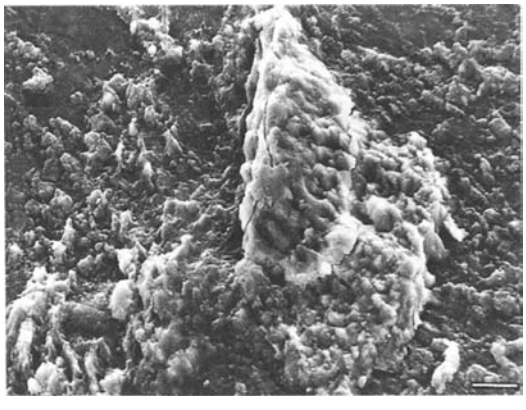

Figure 6 Scanning electron micrograph of an adhesive fracture surface of fracture type 2 (metal bracket, mechanical debonding) with an attached single enamel particle. Bar = 10 μm.

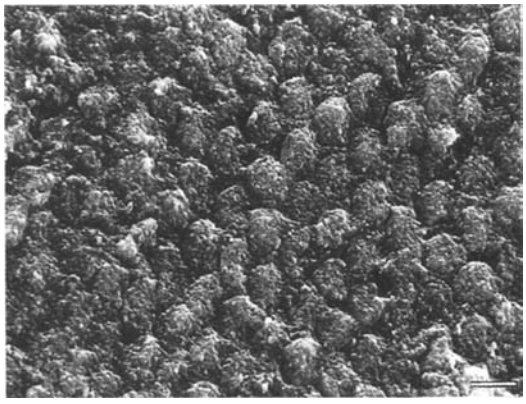

Figure 7 Scanning electron micrograph of an adhesive fracture surface of fracture type 2 (metal bracket, mechanical debonding) with a pattern of disrupted tag residues. Bar = 5 μm.

However, both mechanisms should result in a debonding fracture type, whose interface lies between the adhesive and the bracket base. This theoretical postulation has indeed been supported in a series of metal and ceramic bracket thermodebonding experiments (Sander and Weinrich, 1989; Bishara and Trulove, 1990), in which the percentage of the fracture interface between adhesive and bracket base lay in the range of 85–100 per cent. Likewise, in this investigation we found a high proportion of the so-called fracture type I (79 per cent) after thermodebonding of ceramic brackets. In our opinion the fracture mechanism is based on a reduction of intermolecular binding forces of the adhesive neighbouring the ceramic bracket base due to a localized plastification rather than on structural tensions arising due to rapid thermal expansion.

Our hypothesis is supported by the observation of the adhesive fracture surfaces of fracture type I (see Figure 5), whose smooth and glossy appearance provides morphological evidence of a plastified and rehardened material. However,

Table 4 Computer-aided area analysis of enamel particles and percentage of total particle area related to the total adhesive area after mechanical debonding of metal brackets.

Specimen	Mean area of single enamel particles (μm^2)	Total area of enamel particles (mm^2)	Percentage of enamel particle area
1	2723	4.9	72
2	3667	1.9	38
3	*	2.2	26
4	3849	3.1	41
5	211	3.9	44
6	4343	3.2	28
7	2898	2.5	16
8	4451	5.8	52
9	3204	5.2	48
10	*	2.3	21
11	5376	3.7	23
12	2339	3.1	54
13	*	4.4	39
14	3567	5.1	47
15	*	2.4	17
16	4223	4.5	34
17	2899	5.6	42
19	3453	3.5	34
20	2768	4.2	25

* Single enamel particles could not be detected.

this hypothesis also implies, that the resin's plastification temperature has been surpassed, which for the resin Concise is in the range of 130–180°C (Rueggeberg and Lockwood, 1990). According to Ruppenthal and Baumann (1992) the ceramic debonding unit applied in this study produces a metallic element temperature of approximately 750°C, which is high enough to increase the temperature of the resin at the bracket base above its range of plastification, according to our physical calculations of thermal conductivity and thermal capacity.

For thermodebonding the problem of irreversible pulpal damage due to transferred thermal energy via the resin, the enamel and the dentine is negligible since pulpal heating by more than 5.5°C, which represents the critical rise according to Zach and Cohen (1965), does not occur in *in vitro* experiments (Sander and Weinreich, 1989; Bäzner *et al.*, 1991; Ruppenthal and Baumann, 1992).

After thermodebonding the three other fracture types were found in 21 per cent of the specimens. In the scanning electron micrographs of these adhesive fracture surfaces we could not find any signs of a previous plastification process. These morphological results indicate a reduction or even an absence of resin heating, possibly due to a transitory technical error in the generation of the voltage impulse. The preservation of the resin's structural integrity avoids any local instabilities predisposing to later resin fractures and therefore requires a higher mechanical force for debonding. In case of a fracture interface lying completely or partly between adhesive and enamel surface this mechanical debonding force can cause enamel surface fractures if it exceeds the enamel breaking strength, for which Bowen and Rodriquez (1962) have determined a value of 10.34 ± 1.47 N/mm^2. Indeed our results document a relatively high percentage of enamel particles attached to the adhesive fracture surface (62.5 per cent) in the group of fracture types 2, 3 and 4, which is presumably a consequence of higher mechanical forces applied during thermodebonding.

According to Bäzner *et al.* (1991) a torque of 100 Nmm is recommended for thermodebonding using the ceramic debonding unit. This torque corresponds to a shear force of 10–20 N/mm^2 stressing the bracket–adhesive–enamel–complex and entails a substantial risk of enamel surface fractures. Other authors have detected enamel lesions after exclusively mechanical debonding of ceramic brackets, for which Joseph and Roussouw (1990) found enamel fractures in 40 per cent of the specimens.

In contrast to the high percentage of fracture type 1 after thermodebonding of ceramic brackets, there was a completely different distribution of fracture types after mechanical debonding of metal brackets. Table 1 gives the distribution of debonding fracture types in the group with thermodebonding with only 38 per cent of the investigated specimens showing fracture type 1, whereas almost half of the specimens (45 per cent) had fractured at the interface between adhesive and enamel surface (type 2). Therefore the retentive and the adhesive forces between the resin and the enamel surface or the resin and the bracket base are similar and are both weaker than the cohesive forces of the resin material itself. These conclusions are confirmed by an extensive study by Diedrich (1983), who reported a similar distribution of fracture types and who determined a mean value of 11.2 N/mm^2 for the tensile bond strength between acid etched enamel surface and the resin Concise. For the bond strength between Concise and a metal bracket base, Diedrich (1983) calculated a mean value of 9.8 N/mm^2.

Since mechanically applied forces must exceed one of these bond strength values during the debonding process and since they are of the magnitude of the enamel breaking strength, the risk of enamel surface fractures is high during mechanical debonding. Our morphological and microanalytical evaluations confirm this high risk of enamel surface fractures since enamel particles attached to the adhesive surface were detected in 77 per cent of the specimens belonging to the group of fracture types 2, 3 and 4.

Concerning the size and the extension of the enamel particles, a discrepancy between our results and the avaible data in the literature was noted. In a comprehensive study on mechanical debonding with 163 extracted teeth Diedrich (1981) demonstrated that localized detachments of terraced or ribbed enamel particles occurred more frequently with plastic than with metal brackets. He confirmed these results in a subsequent study (Diedrich, 1983) and observed that whole plates were detached from the enamel surface after mechanical debonding of metal brackets. He measured these plates to have a thickness of up to 100 μm and found areas of approximately 2 mm^2, with a few plates up to 10 mm^2. Fischer-Brandies *et al.* (1993) compared two different methods of bracket debonding and found that the mean area of enamel lesions amounted to 48.3 per cent of the adhesive-free enamel surface when a torsional movement was applied for debonding, whereas bracket debonding by a bending movement produced only superficial and less frequent enamel lesions.

Such discrepancies are not surprising since the geometry of the detached enamel particles is considered to depend on several parameters such as the enamel etching pattern, which may result in the different formation of resin tags (Abendroth and Bößmann, 1979), the type of adhesive and brackets and the technique of debonding.

Future *in vitro* and *in vivo* studies will need to demonstrate the reproducibility of the favourable results of the described thermodebonding technique. Presently a prospective study aimed at determining the significance of different adhesive types and bracket modifications (ceramic brackets versus metal brackets) for standardized clinical application is in progress.

Conclusions

The electrothermal debonding technique in the case of ceramic brackets is predominantly superior to the conventional mechanical debonding technique. The thermodebonding process entails a low risk of enamel surface fracturing since the fracture interface lies between the adhesive and the bracket base in 79 per cent of the specimens. The results of the statistical estimation are given in Table 2. However, this advantage of enamel-protective debonding can dissipate if the accompanying mechanical force for final bracket removal exceeds the value of the enamel breaking strength.

After mechanical debonding of metal brackets almost half of the specimens (45 per cent) showed fractures at the interface between adhesive and enamel surface. In this case only minor residues of adhesive have to be removed from the enamel surface mechanically, which means that bracket removal takes less time in clinical practice. However, thermodebonding is a much safer method because, according to our results, mechanical debonding entails a fourfold risk of enamel surface fracturing (enamel fracture rate = 47.6 per cent) as compared with the

electrothermal debonding technique (enamel fracture rate = 11.9 per cent).

Statistically the expected percentages of the enamel fracture rates were estimated to lie in the range of 23–63 per cent for mechanical debonding and 4–25 per cent for thermodebonding (level of significance $\alpha = 5$ per cent).

Address for correspondence

Dr. Udo Stratmann
Institute of Anatomy
University of Münster
Robert Koch Straße 26
D–48129 Münster, Germany

References

Abendroth R, Bößmann K 1979 Variation der Ätzmuster an Schmelzoberflächen nach Behandlung mit verschiedenen Ätzmitteln. Deutsche Zahnärztliche Zeitschrift 34: 181–184

Bäzner B, Ettwein K H, Röhlcke F, Sernetz F 1991 In-vitro-Untersuchungen zum thermischen Debonding von Keramikbrackets. Fortschritte der Kieferorthopädie 52: 322–333

Bishara S E, Trulove T S 1990 Comparisons of different debonding techniques for ceramic brackets: an *in vitro* study. Part II. Findings and clinical implications. American Journal of Orthodontics and Dentofacial Orthopedics 98: 263–273

Bowen R L, Rodriguez M S 1962 Tensile strength and modulus of elasticity of tooth structure and several restorative materials. Journal of the American Dental Association 64: 378–387

Diedrich P 1981 Enamel alterations from bracket bonding and debonding: a study with the scanning electron microscope. American Journal of Orthodontics and Dentofacial Orthopedics 79: 500–522

Diedrich P 1983 Bracketadhäsivtechnik. Karl Hanser Verlag, München

Douglas J B 1989 Enamel wear caused by ceramic brackets. American Journal of Orthodontics and Dentofacial Orthopedics 95: 96–98

Fischer-Brandies H, Kremers L, Reicheneder C, Kluge G, Häusler K 1993 Über die Schmelzschädigung in Abhängigkeit von der Methode der Bracketentfernung. Fortschritte der Kieferorthopädie 54: 64–70

Gerkhardt K D, Hohmann W, Kocjancic B, Schopf P M 1988 Elektrothermische Bracketentfernung durch Erweichung des Klebers mittels Hochstromimpuls. Praktische Kieferorthopädie 2: 145–148

Hall T A 1971 Microprobe assay of chemical elements. In: Physical techniques in biological research. Vol 1A. Academic Press, New York, pp 157–275

Hertrich K, Hirschfelder U 1990 Erfahrungen erwachsener Patienten mit ihrer kieferorthopädischen Behandlung. Fortschritte der Kieferorthopädie 51: 44–48

Joseph V P, Rossouw E 1990 The shear bond strengths of stainless steel and ceramic brackets used with chemically and light-activated composite resins. American Journal of Orthodontics and Dentofacial Orthopedics 97: 121–125

Jost-Brinkmann P G, Dürr W, Miethke R 1989 Thermodebonding von Metall- und Keramikbrackets. Praktische Kieferorthopädie 3: 249–256

Kusy R P 1988 Morphology of polycrystalline alumina brackets and its relationship to fracture toughness and strength. Angle Orthodontist 58: 197–203

Maskeroni A J, Meyers C E, Lorton L 1990 Ceramic bracket bonding: a comparison of bond strength with polyacrylic acid and phosphoric acid enamel conditioning. American Journal of Orthodontics and Dentofacial Orthopedics 97: 168–175

Newesely H B, Rossiwall I 1989 Schmelzabrasionen und Schmelzausrisse bei Keramikbrackets. Informationen in Orthodontie und Kieferorthopädie 21: 577–594

Ødegaard J, Segner D 1988 Shear bond strength of metal brackets compared with a new ceramic bracket. American Journal of Orthodontics and Dentofacial Orthopedics 94: 201–206

Rueggerberg F A, Lockwood P 1990 Thermal debracketing of orthodontic resins. American Journal of Orthodontics and Dentofacial Orthopedics 98: 56–65

Ruppenthal T, Baumann M A 1992 Zur Temperaturerhöhung in der Zahnpulpa während elektrothermischer Abnahme von Keramikbrackets Fortschritte der Kieferorthopädie 53: 111–116

Ruppenthal T, Stratmann U, Sergl H G, Czech D 1992 Elementanalytische und quantitativ-morphometrische Bestimmung von Kunststoffresten und Schmelzausrissen nach der Abnahme von Metallbrackets. Fortschritte der Kieferorthopädie 53: 99–105

Sander F G, Weinrich A 1989 Sind Keramikbrackets ein Fortschritt für unsere Patienten? Zahnärztliche Mitteilungen 79: 2730–2740

Scott G E 1988 Fracture toughness and surface cracks–the key to understanding ceramic brackets. Angle Orthodontist 58: 5–8

Sheridan J J, Brawley G, Hastings J 1986 Electrothermal debracketing. Part I. An *in vitro* study. American Journal of Orthodontics 89: 21–27

Zach L., Cohen G 1965 Pulp response to externally applied heat. Oral Surgery 19: 515–530